https://doi.org/10.20965/ijat.2022.p0167

Paper:

Quantitative Evaluation of Machined-Surface Gloss Using Visual Simulation and its Application to Sensory Test

Motohiro Ihara, Iwao Yamaji, and Atsushi Matsubara†

Department of Micro Engineering, Graduate School of Engineering, Kyoto University
Kyotodaigaku-katsura, Nishikyo-ku, Kyoto 615-8540, Japan
†Corresponding author, E-mail: matsubara.atsushi.5v@kyoto-u.ac.jp
[Received October 22, 2021; accepted December 21, 2021]

In the machining field, the quality of a machined surface is characterized using both quantitative and sensory parameters. It is important to quantitatively evaluate sensory parameters to automate the evaluation of machined surfaces and determine the machining conditions. In this study, we quantitatively evaluate the gloss degree, which is a sensory parameter, via visual simulation. The gloss degree is evaluated based on an angular luminance distribution for machined surfaces cut using different tools. Using the quantitative evaluation result, observation is conducted to predict the appearance of the machined surface, and a sensory test is performed. The result shows that the quantitative evaluation results are consistent with the sensory test results.

Keywords: machined surface, sensory parameter, quantitative evaluation, gloss, visual simulation

1. Introduction

Methods to automatically determine machining conditions have been investigated to improve the efficiency of the cutting process. Some of these studies are based on the quality of machined surfaces [1–4]. In such methods, quantified parameters, such as surface roughness, are used to determine quality. In general, both quantitative and sensory parameters, such as the gloss degree [5], iridescent surfaces [6, 7], and inhomogeneity, are used to determine the quality of a machined surface. Quantitative evaluation of such sensory parameters is an issue in the automation of machined surface evaluation and machining condition decisions.

In the cutting process, the motion trajectory of the cutting edge of a tool is transferred to the machined surface. If the cutting edge shape of the tool is smooth and the tool motion is accurate, a machining surface shape with a regular pattern (cusp shape) is formed macroscopically. The cusp shape is perceived as a cutting pattern. In reality, minute irregularities of submicron scale exist in the cutting edge, and cutting phenomena such as plastic flow are added, thereby forming not only a macroscopic cusp shape but also a microscopic shape. The authors have previously clarified that microscopic shape affects sensory parameters [8]. To quantify the sensory parameters, the effects of macroscopic and microscopic shapes on visual information must be investigated.

For the visual evaluation of a cut surface, for example, Yonehara et al. measured the gloss value of a cut surface using a gloss meter and investigated the effect of surface roughness on the gloss degree [5]. Sato et al. investigated the effect of the motion error of a machining tool on the appearance of a finished surface [9]. In these studies, the cusp shape is changed based on a machining condition and a motion error, and the microscopic shape cannot be considered an influencing factor.

In general, the effect of the minute shape of a surface on light reflection is analyzed using Beckmann's theory on the scattering of electromagnetic waves [10]. Human visual information includes luminance and color [11]. The authors have previously developed a visual simulation method to calculate luminance and color from shape data, including the microscopic shape of a machined surface based on Beckmann's theory and the mechanism of human vision [12]. The authors aim to quantify sensory parameters by calculating the visual information of a machined surface using the developed method and investigating its distribution.

In this study, we focused on the gloss degree caused by a difference in the microscopic shape. In general, studies to quantify gloss values have been performed extensively. It is known that humans sense gloss when an intense specular reflection light appears on a surface [13]. Parameters with which the gloss is quantified include the glossiness, whereas gloss is evaluated based on the ratio of the intensity of specular reflection light to incident light [14]. In computer graphics, gloss is controlled by manipulating parameters associated with specular reflection [15].

Methods for quantifying the gloss degree vary depending on the macroscopic shape of a surface. Researchers have investigated a method to quantify the gloss degree using the distribution of luminance when the surface is observed in one direction and the macroscopic shape is visible to the naked eye [16–18]. Meanwhile, as a method to evaluate the gloss degree when the macroscopic scale is extremely small and invisible to the naked eye, researchers have proposed plotting the luminance value when the observation angle varies while the incident light

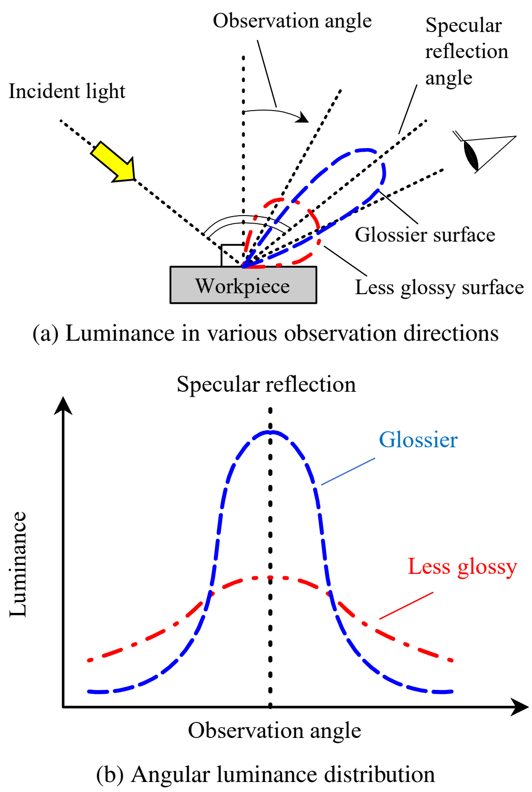

Fig. 1. Difference in angular luminance distribution between glossier and less glossy surfaces.

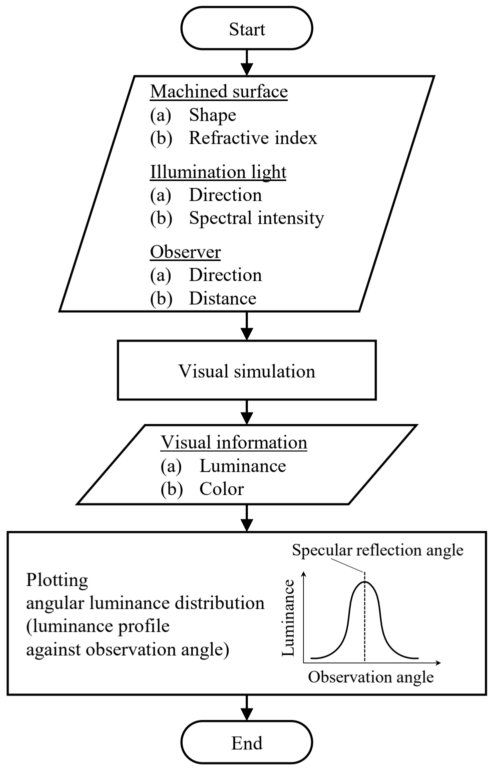

Fig. 2. Procedure for evaluating gloss.

is constant [19]. This luminance curve is known as the angular luminance distribution. When analyzing the gloss of a machined surface, the former method is suitable when the height and width of the cusp shape are sufficient large to be viewed by the naked eye, whereas the latter method is suitable when the scale of the cusp shape is extremely small and not visible to the naked eye.

In this study, luminance was calculated via visual simulation, and the angular luminance distribution was plotted to quantitatively evaluate the gloss degree of machined surfaces cut using different tools. It is noteworthy that we investigated a case involving a cusp shape that was extremely small to be viewed by the naked eye. Quantitative evaluation results were verified via a sensory test.

2. Evaluation Method

According to Hasunuma, when a glossier surface and a less glossy surface are observed from various directions under a fixed illumination light, the angular luminance distributions yielded are different, as shown in **Fig. 1** [19]. The luminance of the glossier surface increases when observed from the direction of specular reflection, whereas the luminance decreases significantly when the observation direction is shifted. Meanwhile, a less glossy surface yields less luminance in specular reflection and less change in luminance with respect to the observation direction. Therefore, it is assumed that the gloss degree can be quantitatively evaluated by investigating the distribution of luminance when observed from various directions, including the direction of specular reflection.

Figure 2 shows a procedure for quantitatively evaluating the gloss degree.

First, the input data for the visual simulation were measured or decided. The shape and refractive index of the machined surfaces were measured. For the illumination, the spectral irradiance was measured, and the direction was determined. For the observer, the distance from the machined surface and the observation direction were determined. Various observation directions were assumed, including the direction of the specular reflection.

Visual simulation was performed using the input data to calculate the visual information at each observation angle. An angular luminance distribution was plotted to evaluate the gloss degree.

3. Cutting Experiment and Quantitative Evaluation

3.1. Purpose

We conducted an experiment to apply the evaluation method to actual machined surfaces. By conducting a cutting experiment using tools with different materials, we prepared surfaces with different gloss degrees and plotted an angular luminance distribution to quantitatively evaluate the gloss degree.

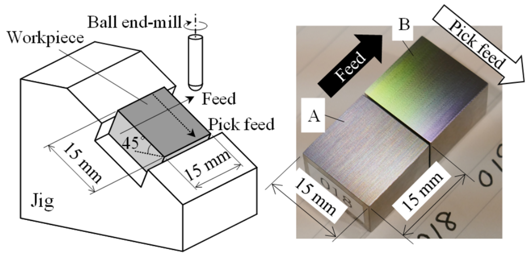

(a) Cutting setup (b) Photograph workpieces

Fig. 3. Cutting setup and photograph of workpieces.

Table 1. Cutting conditions.

Workpiece no.	A	B
Workpiece material	STAVAX (52 HRC)	
Tool material	Coated cemented carbide	cBN
Tool	2-tooth ball end-mill; radius: 1 mm	
Rotation speed	11000 min^{-1}	
Depth of cut	0.05 mm	0.1 mm
Pick feed	0.05 mm	
Feed rate	1100 mm/min	

3.2. Cutting Experiment

In this experiment, workpieces with different gloss degrees were prepared. Therefore, we prepared the same workpiece material via cutting using the ball end-mills of different materials. **Fig. 3(a)** shows the machining setup, and **Table 1** lists the cutting conditions. The workpiece cut using a coated cemented carbide tool is labeled A, and the workpiece cut using a cBN (cubic Boron Nitride) tool is labeled B.

To unify the cusp shape, the pick feed and feed per tooth were set to the same value. In addition, we considered a case in which the cutting pattern was not visible to the naked eye. According to a study by Sato et al., when the observation distance is 250 mm, recognition via the naked eye is impossible when the interval of the cutting pattern becomes smaller than 0.25 mm [20]. In the sensory test performed in this study (as will be discussed in Section 4), the observation distance was set to 15 cm, and it was predicted that a cutting pattern smaller than 0.15 mm could not be recognized. Therefore, we specified the machining condition such that the pick feed and feed per tooth were 0.05 mm. **Fig. 3(b)** shows a photograph of the machined surface. The cutting pattern was extremely fine and hence difficult to identify.

The shapes of workpieces A and B were measured using a white-light interferometer (spatial resolution: 0.3 μm; height measurement resolution: 0.01 nm) at three different areas each, as well as using a contact surface roughness measuring instrument (spatial resolution: 0.1 μm; stylus tip radius: 5 μm; measurement length: 4 mm) at six different lines each along the pick feed direction. The measurement positions of the two methods were not necessarily the same.

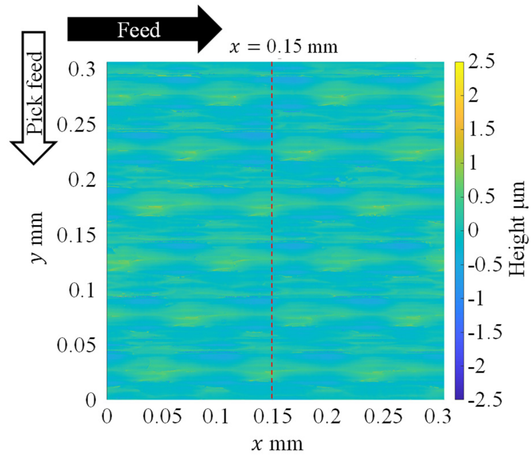

(a) A, area 1 (cemented carbide tool, $Sa = 0.173$ μm)

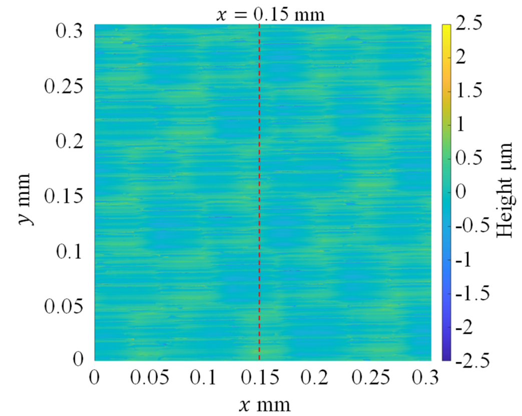

(b) E, area 1 (cBN tool, $Sa = 0.173$ μm)

Fig. 4. Shape data obtained by white-light interferometer.

Figure 4 shows the shape data obtained using the white-light interferometer. **Fig. 5** shows the cross-sectional shapes extracted from the data shown in **Fig. 4** at $x = 0.15$ mm, as well as the roughness profiles obtained using the contact surface roughness measuring instrument. Based on the cutting conditions, the width of the cusp shape was 0.05 mm, and the theoretical cusp height was 0.3 μm, which were difficult to distinguish from **Fig. 5**. However, in both datasets measured via the two methods, the height was 1–2 μm in both workpieces, and the microscopic shapes differed based on the tool material. Hence, the cutting edge shape of the tool and the difference in transferability to the workpiece material were considered.

In the data obtained using the white-light interferometer shown in **Figs. 5(a1)** and **(b1)**, outliers were conspicuous compared with those obtained using the contact measurement instrument shown in **Figs. 5(a2)** and **(b2)**. **Table 2** summarizes the surface roughness Sa calculated using the measurement data obtained using the white-light interferometer, and arithmetic average roughness Ra obtained measured using the contact surface roughness mea-

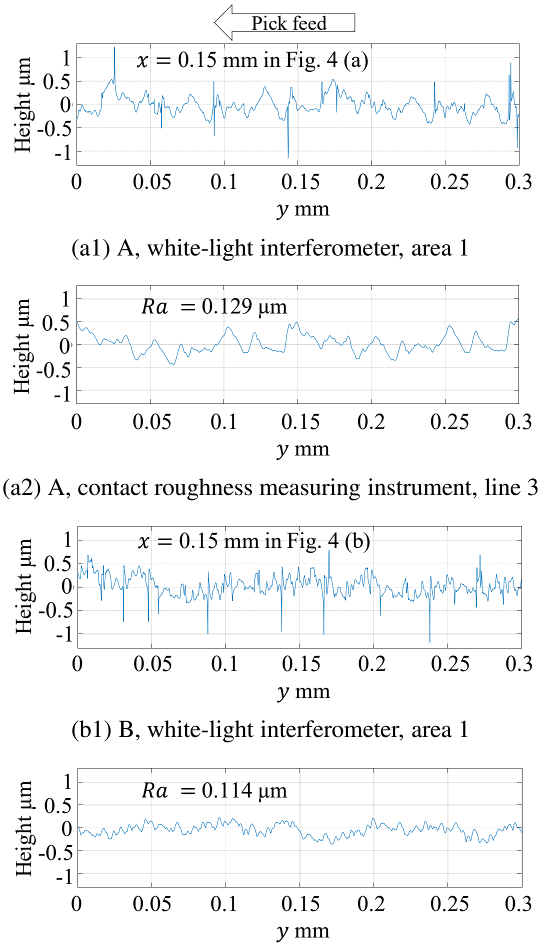

(a1) A, white-light interferometer, area 1

(a2) A, contact roughness measuring instrument, line 3

(b1) B, white-light interferometer, area 1

(b2) B, contact roughness measuring instrument, line 3

Fig. 5. Comparison of roughness profiles measured by contact roughness measuring instrument and cross-sectional shape obtained by white-light interferometer.

Table 2. Summary of *Sa* calculated from measurement data measured using white-light interferometer and *Ra* measured using contact surface roughness measuring instrument.

	Workpiece A	Workpiece B
Sa measured using white-light interferometer	0.168±0.005 μm	0.166±0.007 μm
Ra measured using contact surface roughness measuring instrument	0.157±0.016 μm	0.119±0.008 μm

surement instrument. *Sa* and *Ra* were of the same scale for both workpieces. The gap of *Sa* was smaller than 10%, whereas the *Ra* of B was approximately 30% lower than that of A. Therefore, the differences in the measurement methods should be considered. For example, irregularities smaller than the tip radius cannot be measured accurately using a contact measuring instrument.

The refractive index of the machined surface was measured using a spectroscopic ellipsometer (incident angle:

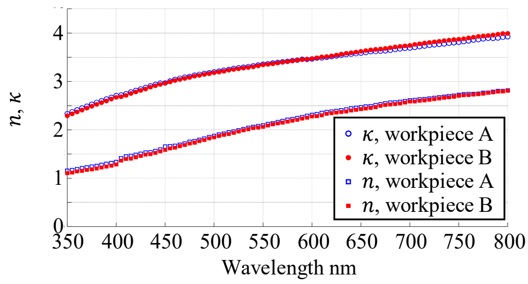

Fig. 6. Measured refractive index.

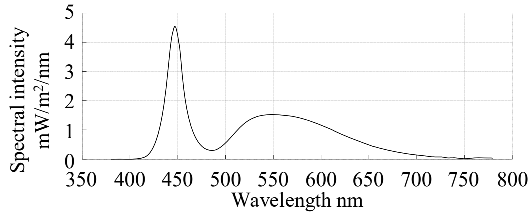

Fig. 7. Measured spectral intensity of LED light source.

70°; measurement wavelength range: 300–1000 nm; measurement wavelength interval: 5 nm). The measurement results are shown in **Fig. 6**. In general, the refractive index of metals is complex [21]. In the figure, n denotes the real component of the refractive index, and κ denotes the extinction coefficient (the imaginary component of the refractive index multiplied by -1). The maximum difference in refractive index was approximately 0.1.

3.3. Quantitative Evaluation of Gloss Degree

The evaluation method described in Section 2 was applied to machined surfaces A and B.

We used shape data measured using the white-light interferometer and the refractive index, as shown in **Figs. 4** and **6**, respectively. For the spectral irradiance of the illumination light, the spectral irradiance of the LED illumination light used for the sensory test (as described in Section 4) was measured using a spectral irradiance instrument (measurement wavelength: 380–780 nm; measurement wavelength interval: 1 nm). The results are shown in **Fig. 7**.

Regarding the direction of the illumination light and observation, we considered a case in which the illumination light was incident perpendicular to the feed direction, as shown in **Fig. 8**, which is consistent with the setup of the sensory test. In the figure, θ_1 represents the incident angle of illumination, θ_2 the observation angle, and D the observation distance. **Table 3** shows the calculation conditions. The direction of illumination was fixed, and the observation direction was varied.

Using the data obtained, visual simulation was performed for each observation angle, and the luminance of the machined surface was calculated. **Fig. 9** shows the angular luminance distributions obtained. The luminance of machined surface A was relatively high at 45° in the

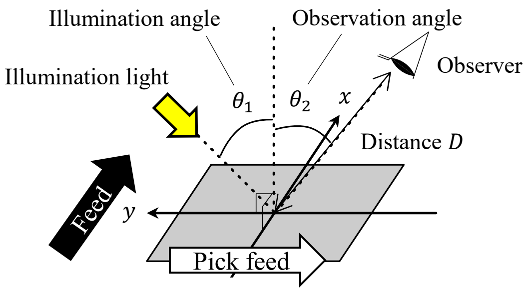

Fig. 8. Definition of illumination and observation angles.

Table 3. Simulation conditions.

Illumination angle θ_1	45°
Observation angle θ_2	20°, 25°, 30°, 35°, 37°, 38°,…, 53°, 55°
Distance D	150 mm

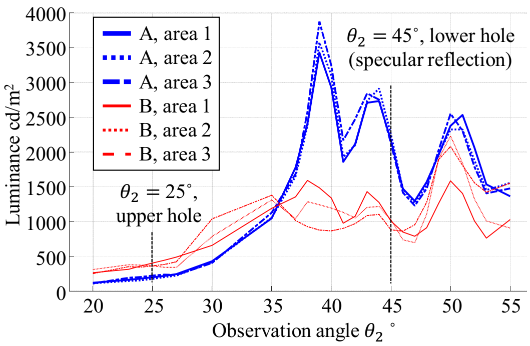

(a) Overall view

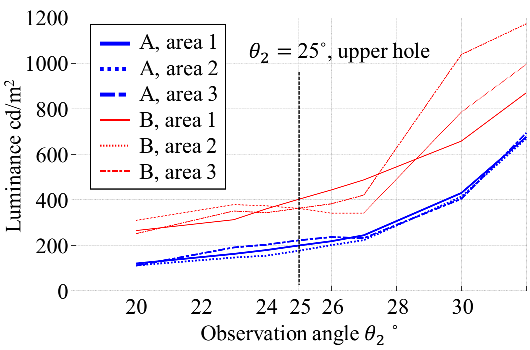

(b) Enlarged view

Fig. 9. Simulated angular luminance distribution.

specular reflection direction, and the luminance of machined surface B was relatively high in the range equal to or less than 30° away from the angle of specular reflection. Therefore, machined surface A had a higher luminance in the specular reflection direction, and the luminance decreased more significantly as the observation angle varied. Hence, machined surface A was evaluated to possess a higher gloss degree.

To determine whether the difference in luminance can be recognized by a human, the luminance contrast threshold was used as a reference. The luminance contrast threshold indicates the degree to which the luminance of an object differs with reference to the background luminance that enables a human to distinguish the background from the object [22]. Although the luminance contrast threshold varies depending on the background luminance, object size, and observation time, the luminance contrast threshold was approximately 10% when the background luminance was on the order of 10^1–10^3 cd/m^2. This indicates that if the luminance of the object differs by approximately 10% with reference to the background luminance, then the object can be distinguished from the background. As an example, in **Fig. 9**, because the difference in luminance at $\theta_2 = 25°$ and 45° exceeds 10% with reference to the value of either machined surface A or B, it is assumed that a human can recognize the difference in luminance. Therefore, it is predicted that the difference in luminance can be clearly recognized when observed at the above-mentioned angles.

3.4. Discussions Regarding Causes of Difference in Gloss Degree

The difference in luminance can be caused by one of two reasons: a difference in the microscopic shape or a difference in the refractive index.

Regarding the refractive index, the difference in the measurement results shown in **Fig. 6** was approximately 5% at the maximum for each n and κ. The Fresnel coefficient and energy reflection coefficient should be calculated to evaluate the effect of the refractive index on luminance. Meanwhile, the Fresnel coefficients for p and s polarizations, i.e., R_p and R_s, respectively, can be obtained as follows [21]:

$$R_p = \frac{\tan(\Theta_{in} - \theta_c)}{\tan(\Theta_{in} + \theta_c)} \quad \dots \dots \dots \dots \quad (1)$$

$$R_s = \frac{-\sin(\Theta_{in} - \theta_c)}{\sin(\Theta_{in} + \theta_c)} \quad \dots \dots \dots \dots \quad (2)$$

Here, Θ_{in} is the incidence angle, and n_0 is the refractive index of air. In addition, n_c is a complex refractive index, and θ_c is a complex refractive angle, which can be obtained as follows:

$$n_c = n - i\kappa \quad \dots \dots \dots \dots \quad (3)$$

$$n_0 \sin\Theta_{in} = n_c \sin\theta_c \quad \dots \dots \dots \dots \quad (4)$$

The Fresnel coefficient at each wavelength was calculated using $n_0 = 1$ and $\Theta_{in} = 45°$. **Fig. 10** shows the square of the absolute value of the calculated Fresnel coefficient, i.e., the energy reflection coefficient. The difference in the energy reflection coefficient was less than 2%, whereas that of machined surface B was higher. Therefore, considering only the effect of the refractive index, the luminance is expected to be approximately 2% higher at the maximum in machined surface B. However, as shown by the angular luminance distribution in **Fig. 9**, the difference was approximately twice the expected value; in

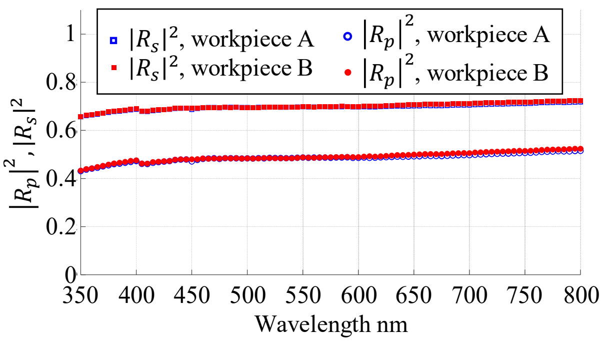

Fig. 10. Calculated energy reflection coefficient.

addition, at some observation angles, the magnitude relationship of luminance was reversed. Therefore, the difference in the microscopic shape shown in **Fig. 5** can be considered as the main contributor to the difference in the gloss degree.

4. Sensory Test Questionnaire Survey

4.1. Questionnaire Method and Results

To verify the quantitative evaluation results, we conducted a questionnaire survey on the sensory tests. The evaluators were nine students in their 20s who majored in mechanical engineering. After explaining about gloss to the evaluators, they were then instructed to observe the machined surfaces based on two types of observation setups (as shown in **Fig. 11**). First, the evaluators were instructed to observe the machined surface based on setup 1 (shown in **Fig. 11(a)**), and then based on setup 2 (shown in **Fig. 11(b)**). Similar to the two setups, a workpiece tilted by 45° was illuminated with an LED, and the workpiece was covered with a black cloth to eliminate the effect of laboratory illumination.

For setup 1, they observed the workpiece from a free angle and answered the question, "which of the machined surfaces appear glossier?" In setup 2, a screen was installed to unify the observation angle, and the workpiece was observed from upper and lower holes. The observation angle was set in the direction of $\theta_2 = 25°$ and 45°, in which the difference in luminance was expected to be clearly recognizable based on the quantitative evaluation results in Section 3.3. The upper hole was set in the direction of $\theta_2 = 25°$, i.e., approximately 20° away from the specular reflection, whereas the lower hole was set in the direction of $\theta_2 = 45°$, i.e., specular reflection.

The evaluators were instructed to answer the question, "which surface appears brighter?" when they were observing through the two holes.

Table 4 shows the results of the sensory test along with the quantitative evaluation results described in Section 3.3. For setup 1, more evaluators answered that machined surface B was glossier. Meanwhile, in setup 2, more evaluators answered that machined surface B appeared brighter based on observation from the upper hole.

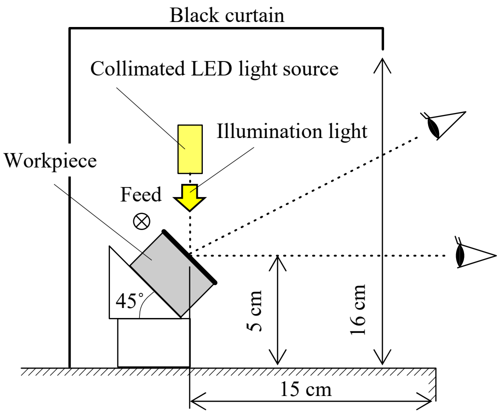

(a) Setup 1, without partition

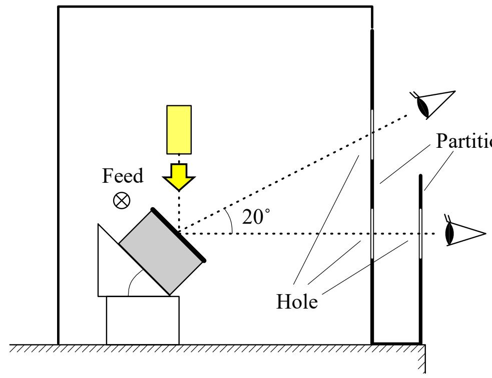

(b) Setup 2, with partition

Fig. 11. Setup of sensory test.

Table 4. Result of sensory test.

	A	B	Quantitative evaluation
Setup 1 "Which appears glossier?"	3	6	A
Setup 2 "Which appears brighter from upper hole?" ($\theta_2 = 25°$)	1	8	B
Setup 2 "Which appears brighter from lower hole?" ($\theta_2 = 45°$)	7	2	A

More evaluators answered that machined surface A appeared brighter based on observation from the lower hole.

4.2. Comparison Between Sensory Test and Quantitative Evaluation Results

In the sensory test based on setup 1, more evaluators answered that machined surface B was glossier; however, the quantitative evaluation results indicate that the gloss degree of machined surface A was higher. To visually evaluate the gloss degree based on setup 1, the machined surface must be observed in both the direction of specular reflection and away from it, after determining the angle of illumination light and the tilt of the machined surface. However, the degree of freedom of the observation direction might be high; as such, the evaluators might not necessarily conduct such observations. For example, machined surface B might exhibit a relatively high gloss degree because it appeared brighter when observed at an angle away from the specular reflection.

In the sensory test based on setup 2, more evaluators answered that machined surface B was brighter as observed through the upper hole, whereas more evaluators answered that machined surface A was brighter as observed through the lower hole. These results are consistent with the calculation result of the angular luminance distribution shown in **Fig. 9**.

5. Conclusions

In this study, we quantitatively evaluated the gloss degree by calculating the luminance of the cut surface using visual simulation and examining the angular luminance distribution plotted for the case where the cutting pattern was extremely fine and not visible to the naked eye.

By cutting STAVAX using ball-end mills of cemented carbide and cBN in a cutting experiment, we prepared machined surfaces with different gloss degrees and applied the quantitative evaluation method. The results showed that the gloss degree of the machined surface using the cemented tool was relatively high.

To validate the quantitative evaluation results, a sensory test was performed. The results showed the results of the sensory test and the quantitative evaluation for both observation setups were consistent, in which the difference in luminance of the machined surfaces was predicted to be clearly recognizable.

It was assumed that the gloss degree differed because the microscopic shapes of the machined surfaces varied depending on the difference in the cutting edge shapes of the tools and their transferability to the workpiece material.

To evaluate the gloss of various machined surfaces, cases where the cutting pattern is large and visible to the naked eye should be investigated in the future.

Acknowledgements

This study was supported by the Mori Manufacturing Research and Technology Foundation. The cutting experiment was supported by Mr. Katsuji Fujii and Dr. Takeshi Watanabe of NS Tool Co., Ltd., and Mr. Tsuneto Sumida and Mr. Shotaro Tanaka of Yasuda Precision Tools K.K. The shape measurement using a white-light interferometer was supported by Mr. Masataka Yauchi of Big Daishowa Seiki Co., Ltd. The measurement of the refractive index using the spectroscopic ellipsometer was supported by the Kyoto Prefectural Technology Center for Small and Medium Enterprises.

References:

[1] H. Oktem, T. Erzurumlu, and H. Kurtaran, "Application of response surface methodology in the optimization of cutting conditions for surface roughness," J. Materials Proc. Tech., Vol.170, pp. 11-16, doi: 10.1016/j.jmatprotec.2005.04.096, 2005.

[2] B. Umroh, Muhathir, and Darianto, "The Optimum Cutting Condition when High Speed Turning of Aluminum Alloy using Uncoated Carbide," 2019 IOP Conf. Ser.: Mater. Sci. Eng. Vol.505, 012041, doi: 10.1088/1757-899X/505/1/012041, 2019.

[3] M. Mia, P. R. Dey, M. S. Hossain, M. T. Arafat, M. Asaduzzaman, M. S. Ullah, and S. M. Tareq Zobaer, "Taguchi S/N based optimization of machining parameters for surface roughness, tool wear and material removal rate in hard turning under MQL cutting condition," Measurement, Vol.122, pp. 380-391, doi: 10.1016/j.measurement.2018.02.016, 2018.

[4] S. Yamashita, T. Furuki, H. Kousaka, T. Hirogaki, E. Aoyama, K. Inaba, and K. Fujiwara, "Investigation of Optimum Grinding Condition Using cBN Electroplated End-Mill for CFRP Machining," Int. J. Automation Technol., Vol.15, No.1, pp. 4-16, doi: 10.20965/ijat.2021.p0004, 2021.

[5] M. Yonehara, K. Kitahara, Y. Kagawa, H. Isono, and T. Sugibayashi, "Effect of topography on glossiness and surface color for a 5052 aluminum alloy," J. Japan Institute of Light Metals, Vol.55, No.1, pp. 15-19, doi: 10.2464/jilm.55.15, 2005.

[6] S. Fujimoto, T. Aizawa, and H. Suyama, "Study on Iridescent Surface," J. Japan Soc. of Prec. Eng., Vol.32, No.6, pp. 409-413, doi: 10.2493/jjspe1933.32.409, 1966.

[7] S. Fujimoto, "Microscopic Gloss of White Iridescent Surface," J. Japan Soc. of Prec. Eng., Vol.41, No.8, pp. 758-763, doi: 10.2493/jjspe1933.41.758, 1973.

[8] M. Ihara, I. Yamaji, and A. Matsubara, "On Classification and Quantification of Sensory Parameters in Judging Mirror Surface: Appearance of a Turned Aluminum Alloy Surface," Proc. of the 2020 Int. Symp. on Flexible Automation, 2020 Int. Symp. on Flexible Automation, V001T08A001, doi: 10.1115/ISFA2020-9607, 2020.

[9] R. Sato, Y. Sato, K. Shirase, G. Campatelli, and A. Scippa, "Finished Surface Simulation Method to Predicting the Effects of Machine Tool Motion Errors," Int. J. Automation Technol., Vol.8, No.6, pp. 801-810, doi: 10.20965/ijat.2014.p0801, 2014.

[10] P. Beckmann and A. Spizzichino, "The Scattering of Electromagnetic Waves from Rough Surfaces," Artech House, Inc., Vol.22, 1987.

[11] K. Ukai, A. Hanazawa, K. Koga, K. Shinomori, K. Uchikawa, and M. Sato, "Vision I," Tokyo, Asakura Publishing, Co., Ltd., 2007 (in Japanese).

[12] M. Ihara, I. Yamaji, K. Fujii, T. Watanabe, M. Yauchi, and A. Matsubara, "Development of a Visual Simulation Method for Quantifying Sensory Evaluation of Machined Surface," J. the Japan Soc. Prec. Eng., Vol.87, No.11, pp. 894-902, doi: 10.2493/jjspe.87.894, 2021.

[13] A. C. Chadwick and R. W. Kentridge, "The perception of gloss: A review," Vision Res., Vol.109, pp. 221-235, doi: 10.1016/j.visres.2014.10.026, 2015.

[14] ISO2813: 2014, "Paints and varnishes – Determination of gloss value at 20°, 60° and 85°," 2014.

[15] Comput. Graphic Arts Soc., "Computer Graphics," Tokyo, Comput. Graphic Arts Soc., 2015 (in Japanese).

[16] H. Komatsu, "Science of Texture," Tokyo, Asakura Publishing, Co., Ltd., 2016 (in Japanese).

[17] A. Nishio, T. Shimokawa, N. Goda, and H. Komatsu, "Perceptual Gloss Parameters Are Encoded by Population Responses in the Monkey Inferior Temporal Cortex," J. Neuroscience, Vol.34, No.33, pp. 11143-11151, doi: 10.1523/JNEUROSCI.1451-14.2014, 2014.

[18] I. Motoyoshi, S. Nishida, L. Sharan, and E. Adelson, "Image statistics and the perception of surface qualities," Nature Letters, Vol.447, pp. 206-209, doi: 10.1038/nature05724, 2007.

[19] H. Hasunuma, "Gloss," Tokyo, Corona Publishing, Co., Ltd., 1960 (in Japanese).

[20] Y. Sato, T. Nakanishi, R. Sato, K. Shirase, M. Oda, and N. Nakayama, "Study on the evaluation method for finished surface based on human visual characteristic," Proc. of 2016 Int. Symp. on Flexible Automation (ISFA2016), pp. 428-431, doi: 10.1109/ISFA.2016.7790201, 2016.

[21] T. Yatagai, "Optics," Tokyo, Asakura Publishing, Co., Ltd., 2017 (in Japanese).

[22] CIE, "An Analytic Model for Describing the Influence of Lighting Parameters Upon Visual Performance (2nd Ed.)," CIE Publishing, 1981.

Name:
Motohiro Ihara

Affiliation:
Graduate School of Engineering, Kyoto University

Address:
Room #c1N06, Building C3, Cluster C, Kyotodaigaku-katsura, Nishikyo-ku, Kyoto 615-8540, Japan

Brief Biographical History:
2017- Master Course Student, Graduate School of Engineering, Kyoto University
2019- Doctor Course Student, Graduate School of Engineering, Kyoto University

Main Works:
• "Development of a Visual Simulation Method for Quantifying Sensory Evaluation of Machined Surface," J. Japan Soc. Prec. Eng., Vol.87, No.11, pp. 894-902, 2021.

Membership in Academic Societies:
• Japan Society for Precision Engineering (JSPE)
• Japan Society of Mechanical Engineers (JSME)

Name:
Iwao Yamaji

Affiliation:
Technician, Department of Micro Engineering, Kyoto University

Address:
Room #c1S09, Building C3, Cluster C, Kyotodaigaku-katsura, Nishikyo-ku, Kyoto 615-8540, Japan

Brief Biographical History:
1983- Engineer, Japan National Railways
1986- Technical Official, Kyoto University
2000- Chief Technical Official, Kyoto University

Main Works:
• "On the removal of critical cutting regions by trochoidal grooving," Precision Engineering, Vol.34, No.3, pp. 467-473, 2010.

Membership in Academic Societies:
• Japan Society for Precision Engineering (JSPE)
• Japan Society for Abrasive Technology (JSAT)
• Society of Automotive Engineers of Japan (JSAE)

Name:
Atsushi Matsubara

Affiliation:
Professor, Department of Micro Engineering, Kyoto University

Address:
Room #c1S07, Building C3, Cluster C, Kyotodaigaku-katsura, Nishikyo-ku, Kyoto 615-8540, Japan

Brief Biographical History:
1992- Research Associate, Kyoto University
2002- Associate Professor, Kyoto University
2005- Professor, Kyoto University

Main Works:
• "Non-contact measurement of spindle stiffness by using magnetic loading device," Int. J. Mach. Tools Manuf., Vol.71, pp. 20-25, 2013.
• "Design of a support system with a pivot mechanism for suppressing vibrations in thin-wall milling," CIRP Ann. – Manuf. Technol., Vol.66, No.1, pp. 381-384, 2017.

Membership in Academic Societies:
• International Academy for Production Engineering (CIRP), Fellow
• Japan Society for Precision Engineering (JSPE)
• Japan Society of Mechanical Engineers (JSME)
• Japan Society for Abrasive Technology (JSAT)